

An abstract drawing from the 73,000-year-old levels at Blombos Cave, South Africa

Christopher S. Henshilwood^{1,2*}, Francesco d'Errico^{1,3}, Karen L. van Niekerk¹, Laure Dayet^{3,4}, Alain Queffelec³ & Luca Pollarolo^{5,6}

Abstract and depicitive representations produced by drawing—known from Europe, Africa and Southeast Asia after 40,000 years ago—are a prime indicator of modern cognition and behaviour¹. Here we report a cross-hatched pattern drawn with an ochre crayon on a ground silcrete flake recovered from approximately 73,000-year-old Middle Stone Age levels at Blombos Cave, South Africa. Our microscopic and chemical analyses of the pattern confirm that red ochre pigment was intentionally applied to the flake with an ochre crayon. The object comes from a level associated with stone tools of the Still Bay techno-complex that has previously yielded shell beads, cross-hatched engravings on ochre pieces and a variety of innovative technologies^{2–5}. This notable discovery pre-dates the earliest previously known abstract and figurative drawings by at least 30,000 years. This drawing demonstrates the ability of

early *Homo sapiens* in southern Africa to produce graphic designs on various media using different techniques.

Blombos Cave (BBC) is situated on the southern Cape coast, about 300 km east of Cape Town (34° 24' 51" S, 21° 13' 19" E). Excavations commenced in 1991 and are on-going. The site contains well-stratified Middle Stone Age (MSA) deposits dating to between 100 and 72 thousand years ago (ka)⁶, topped by a layer of sterile aeolian dune sand (dated to 70 ka) and Later Stone Age layers dated to 2 ka (Fig. 1). The MSA sequence consists of four phases, of which the upper two—'BBC M1' and 'BBC M2 upper'—are associated with the Still Bay techno-complex, dated to about 77–73 ka⁷. These phases contain bifacial foliate points, of which 12% were heated before final shaping using pressure flaking^{5,8}. Other cultural markers of the Still Bay from these layers include bone awls and spear points⁴, possible engravings of parallel and joining lines

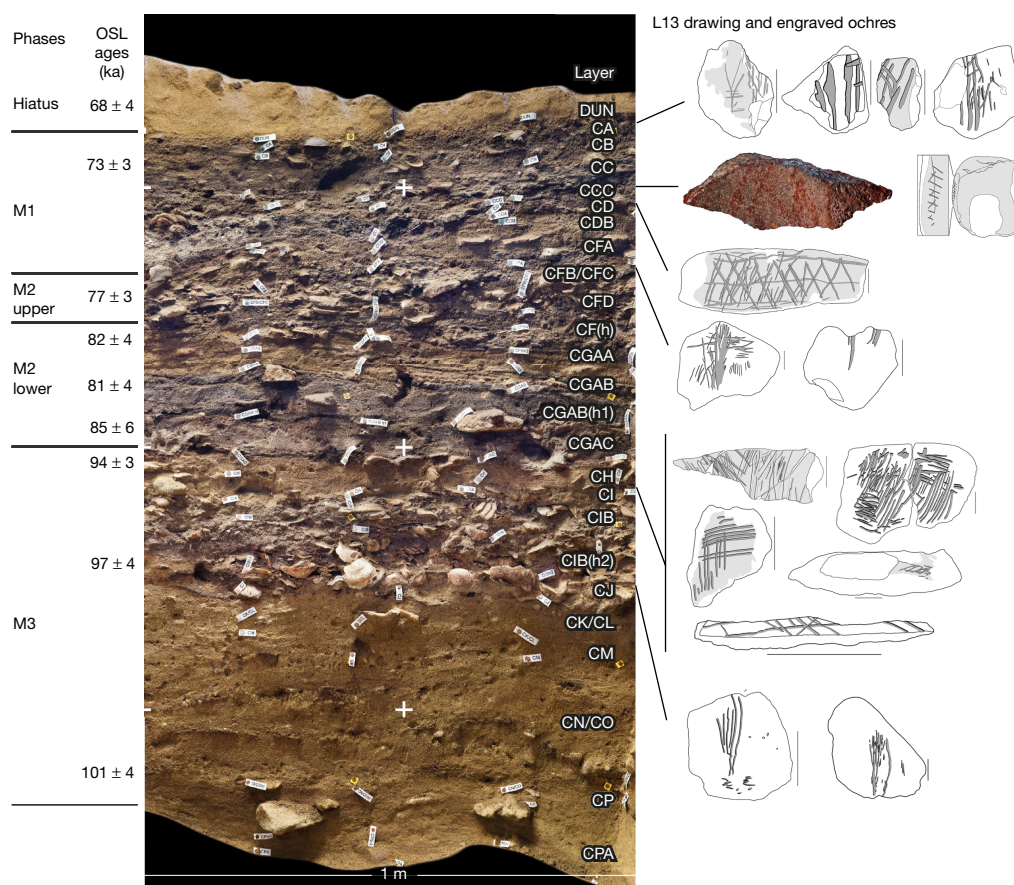


Fig. 1 | Stratigraphy of the south section of Blombos Cave. Left, phases and optically stimulated luminescence dates for the Middle Stone Age levels at Blombos Cave. Centre, labels for individual layers superimposed

on section. Right, layers from which the L13 silcrete flake with ochre drawings and previously described engraved ochre pieces were recovered. Scale bars, 1 cm.

¹SFF Centre for Early Sapiens Behaviour (SapienCE), University of Bergen, Bergen, Norway. ²Evolutionary Studies Institute, University of the Witwatersrand, Johannesburg, South Africa. ³CNRS UMR 5199, University of Bordeaux, Bordeaux, France. ⁴Laboratoire TRACES UMR 5608, Université Toulouse Jean Jaures, Toulouse, France. ⁵Unité d'Anthropologie/Laboratoire Archéologie et Peuplement de l'Afrique, Geneva, Switzerland. ⁶School of Geography, Archaeology and Environmental Studies, University of the Witwatersrand, Johannesburg, South Africa. *e-mail: christopher.henshilwood@uib.no



Fig. 2 | Image of the Blombos Cave silcrete flake L13 displaying the drawn lines that form a cross-hatched pattern. Image credit, C. Foster.

on bone^{4,9}, beads made from *Nassarius kraussianus* shells (67 recovered thus far, some of which are stained with ochre^{3,10}) and pieces of ochre engraved with geometric patterns, eight of which have been recovered thus far—of which two display distinct cross-hatched designs^{2,11}.

The 'M2 lower' phase (dated to about 85–82 ka) is a low-intensity occupational horizon with no Still Bay type artefacts or engraved ochre. The M3 phase (dated to about 101–94 ka) contains abundant natural and used ochre, as well as ten pieces of ochre engraved with geometric designs that include three crosshatched motifs¹¹. In addition, an in situ toolkit consisting of ochre, heated seal bone, charcoal and associated processing materials—used to create a liquid pigmented compound stored in abalone shells—was recovered from a layer of this phase that dates to about 100 ka⁶.

The silcrete flake with a cross-hatched pattern described here was excavated in 2011 and comes from the M1 phase (layer CCC, square G7b). The objects recovered from this layer were gently washed with running tap water in the field and the laboratory, and dried at air temperature. The pattern on the piece was noticed during analysis of the lithic debitage. The piece was numbered L13 in the laboratory (Fig. 2, Supplementary Data and Supplementary Video). The flake is coarse-grained silcrete (length 38.6 mm, width 12.8 mm and height 15.4 mm). The pattern is on a slightly concave smooth face—the flake's striking platform—and extends to a flake scar on the same surface. It consists of a set of six straight sub-parallel lines (Fig. 3, lines 1–6) crossed obliquely by three slightly curved lines (lines 7–9). Line 6 partially overlaps the edge of the flake scar, which suggests it was made after the flake became detached. All the lines are discontinuous and one (line 5) is wider and better defined than the others. Microscopic and chemical analyses confirm that the lines on L13 are composed of haematite-rich powder, commonly called ochre (Extended Data Fig. 1, Supplementary Information and Supplementary Table 2). They differ markedly in colour and composition from the silcrete and the orange calcite patches present on the same surface. The abrupt termination of all lines on the fragment edges indicates that the pattern originally extended over a larger surface (Fig. 3b)—the pattern was probably more complex and structured in its entirety than in this truncated form.

Experimentally marking silcrete flakes with ochre crayons or paint indicates that the lines on L13 were produced with a crayon and thus constitute a drawing (Fig. 4, Extended Data Figs. 3, 4, Supplementary Information and Supplementary Table 1). Discontinuous lines consisting of loose powder in recesses and firmly adhering ochreous patches on elevated areas are produced when experimentally marking a silcrete flake with an ochre crayon. Parallel striations are visible on the patches. These same diagnostic features are seen on the lines composing the pattern on L13. By contrast, our experimental painted lines have clear edges, are solidly filled and show no striations (Extended Data Fig. 7a). The deposits produced by the two techniques are still clearly visible on the experimental material after rinsing under running water (Extended Data Fig. 7c).

The width of the lines on the archaeological material, compared to their experimental counterpart, indicates that they were probably drawn with a pointed ochre crayon (Extended Data Fig. 5). Lines 2, 3, 4, 7, 8 and 9 were made by a single stroke with a 1.3–3.3-mm-wide ochre tip. Line 5 is wider and the ochre is more continuous, probably because it was created with multiple strokes. On experimental drawn lines, loose powder followed by a compacted streak is an indicator of

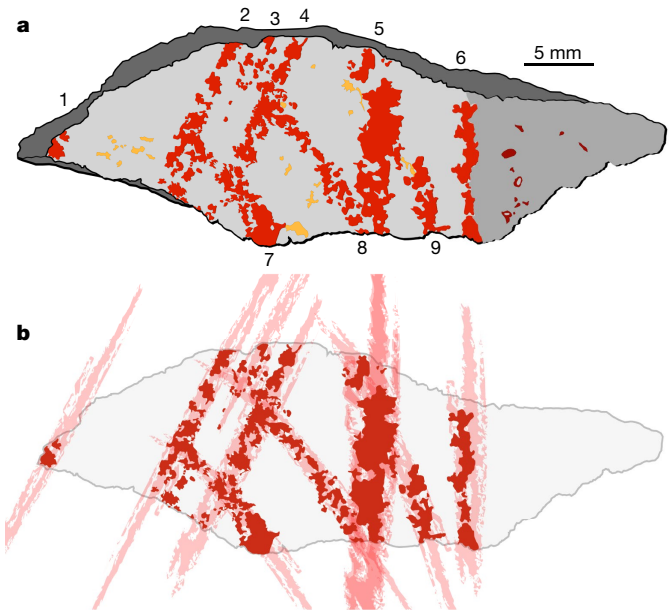


Fig. 3 | Renditions of L13. a, Tracing with the drawn red lines numbered, the calcite patches shown in orange and the ochre residues in dark red. The ground surface is coloured light grey, the darker grey area indicates a flake scar and the darkest grey indicates the breakage fractures after L13 became detached from the originally larger grindstone. **b**, Schematic of lines extending beyond the outline of the present flake.

stroke direction. When applied to the L13 drawing, this observation shows that the single-stroke lines 2, 3 and 4 were drawn in the same direction (Extended Data Figs. 3, 4). Line 5 is a multiple-stroke line, perhaps produced by a to-and-fro motion (Fig. 3). Line 6 does not show clear indication of directionality. Line 8—and probably lines 7 and 9—was drawn in a direction opposite to that of lines 2, 3 and 4, which could indicate that the object was turned during drawing. The order in which the lines were drawn could not be established.

The surface on L13 with the drawing is smoothed by grinding and shows microscopic haematite-rich residues, which indicates that the object is a flake from a grindstone that was used to process ochre before the drawing was made (Extended Data Fig. 2). Subsequent cleaning of the grindstone by the inhabitants of BBC removed most traces of loose ochre powder (produced during grinding), and left a surface that was almost clean but which retained minute traces of ochre. Tribological analysis conducted with two different methods supports the grindstone hypothesis; it shows that the surface with the drawing is significantly smoother than the other faces of L13 and typical cortical and knapped surfaces of other pieces of silcrete recovered from MSA levels at BBC, which confirms that the smoothing recorded on L13 cannot be due to natural processes (Extended Data Fig. 6a, b, Supplementary Information and Supplementary Table 3).

Experimental reproduction of the lines found on L13 using the same technique (that is, using a pointed ochre crayon) indicates that the drawing was more visible when it was produced and that the loose powder that originally composed the lines was subsequently lost through taphonomic processes and rinsing. The lines produced on smooth silcrete—such as on L13—are better defined than on rough surfaces; and the ochre crayon used for the design was probably soft and produced lines that adhered well to the silcrete. We conclude that the ochre crayon was intentionally used to produce a cross-hatched design.

Ochre powder was used for practical purposes by MSA people; for example, as a glue additive and perhaps as a sun screen^{12,13}. Experimental reproduction of numerous lines longer than all those on L13 (Extended Data Fig. 3b, Supplementary Information) produced less than 1 mg of ochre powder, thus discounting a utilitarian objective for the production of the L13 lines.

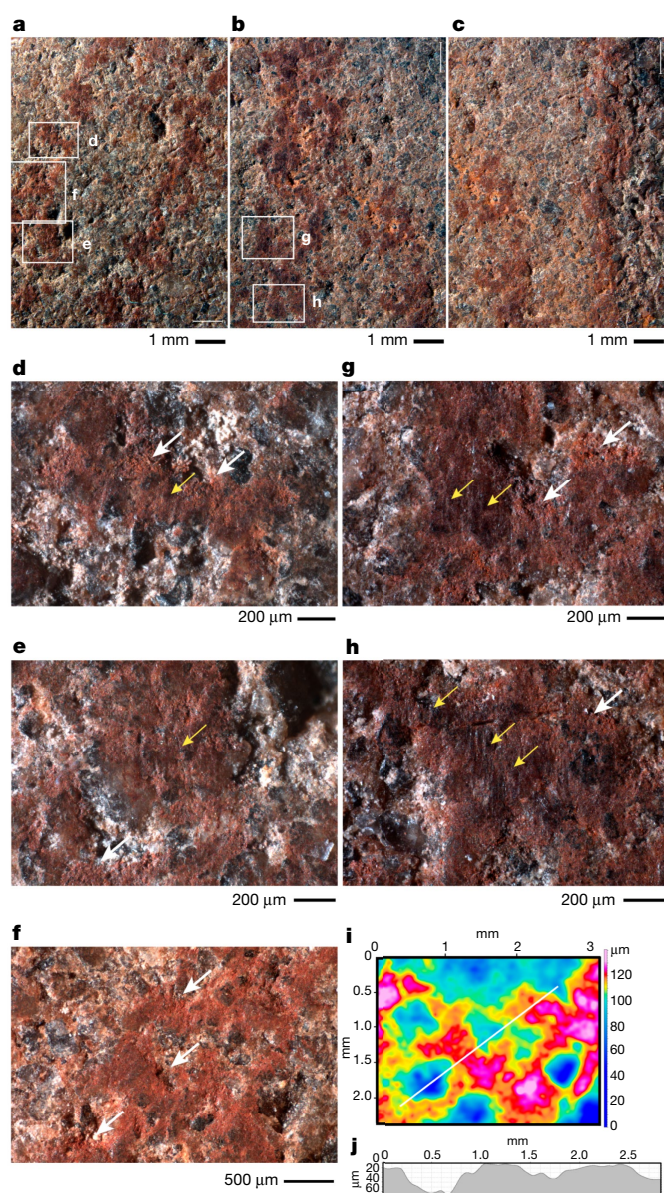


Fig. 4 | Close-up views of the drawn lines on the L13 surface. a, Middle portions of lines 3 and 4 with location of the micrographs shown in d–f. b, Lines 8 and 9 on the proximal portion of the flake, with location of the micrographs g, h. c, Lines 9 and 6 on the proximal portion of the flake. i, Depth map of micrograph shown in f, with the location of the section shown in j indicated by a white line. Large white large arrows (d–h) point to deposits of powdery ochre preserved in recesses, small yellow arrows (d, e, g, h) point to prominent areas with compacted ochre deposits on which remnants of striations are still visible. These features are similar to those produced when a silcrete flake is experimentally marked with an ochre crayon (Extended Data Fig. 3b).

Abstract engravings are known from several archaeological sites that pre-date the Later Stone Age (which began about 42–44 ka) in Africa, and from the Upper Palaeolithic (dated to about 44 ka) in Europe; these include an engraved shell from Trinil dated to 540 ka¹⁴, an engraved bone from Bilzingsleben at 370 ka¹⁵, engraved ochre from BBC (100–73 ka)¹¹, engraved cortices from Qafzeh (90 ka)¹⁶ and Quneitra (60 ka)¹⁷, engraved ostrich egg shells from Diepkloof¹⁸ and Klipdrift Shelter (65–59 ka)¹⁹ and engraved bedrock from Gorham's Cave (over 40 ka)²⁰. A date of 66–64 ka—which would indicate Neanderthal authorship—has recently been proposed for ochre markings from three caves in Spain^{21,22}. However, the earliest previously known evidence for drawing techniques comes from much younger

sites that post-date 42 ka, such as Chauvet^{23,24}, El Castillo²⁵, Apollo 11²⁶ and Maros caves²⁷.

The discovery of L13 demonstrates that drawing was part of the behavioural repertoire of populations of early *Homo sapiens* in southern Africa at about 73 ka. It demonstrates their ability to apply similar graphic designs on various media using different techniques. The discovery of abstract engravings on ochre, with patterns comparable to L13, from levels at BBC dated to 100–73 ka (Fig. 1) and the production of an ochre-rich paint stored in abalone shells⁶ suggest that drawings and possibly paintings may have been produced in older MSA levels, perhaps since 100 ka. The cross-hatched pattern of L13 pre-dates by at least 30,000 years the earliest previously known abstract and figurative drawings. This finding supplements previous evidence reflecting cultural modernity and symbol use that has already been identified in the MSA levels at BBC through the discovery of personal ornaments, elaborate bone tools, engravings, and the production and storage of pigmented compounds. The L13 drawing adds a further dimension to our understanding of the processes that shaped the behaviour and cognition of early *H. sapiens*.

Online content

Any methods, additional references, Nature Research reporting summaries, source data, statements of data availability and associated accession codes are available at <https://doi.org/10.1038/s41586-018-0514-3>.

Received: 16 February 2018; Accepted: 7 August 2018;

Published online: 12 September 2018

- d'Errico, F. & Stringer, C. B. Evolution, revolution or saltation scenario for the emergence of modern cultures? *Phil. Trans. R. Soc. Lond. B* **366**, 1060–1069 (2011).
- Henshilwood, C. S. et al. Emergence of modern human behavior: Middle Stone Age engravings from South Africa. *Science* **295**, 1278–1280 (2002).
- Henshilwood, C., d'Errico, F., Vanhaeren, M., van Niekerk, K. & Jacobs, Z. Middle Stone Age shell beads from South Africa. *Science* **304**, 404 (2004).
- d'Errico, F. & Henshilwood, C. S. Additional evidence for bone technology in the southern African Middle Stone Age. *J. Hum. Evol.* **52**, 142–163 (2007).
- Mourre, V., Villa, P. & Henshilwood, C. S. Early use of pressure flaking on lithic artifacts at Blombos Cave, South Africa. *Science* **330**, 659–662 (2010).
- Henshilwood, C. S. et al. A 100,000-year-old ochre-processing workshop at Blombos Cave, South Africa. *Science* **334**, 219–222 (2011).
- Jacobs, Z., Hayes, E. H., Roberts, R. G., Galbraith, R. F. & Henshilwood, C. S. An improved OSL chronology for the Still Bay layers at Blombos Cave, South Africa: further tests of single-grain dating procedures and a re-evaluation of the timing of the Still Bay industry across southern Africa. *J. Archaeol. Sci.* **40**, 579–594 (2013).
- Villa, P., Soressi, M., Henshilwood, C. S. & Mourre, V. The Still Bay points of Blombos Cave (South Africa). *J. Archaeol. Sci.* **36**, 441–460 (2009).
- d'Errico, F., Henshilwood, C. S. & Nilssen, P. An engraved bone fragment from c. 70,000-year-old Middle Stone Age levels at Blombos Cave, South Africa: implications for the origin of symbolism and language. *Antiquity* **75**, 309–318 (2001).
- Vanhaeren, M., d'Errico, F., van Niekerk, K. L., Henshilwood, C. S. & Erasmus, R. M. Thinking strings: additional evidence for personal ornament use in the Middle Stone Age at Blombos Cave, South Africa. *J. Hum. Evol.* **64**, 500–517 (2013).
- Henshilwood, C. S., d'Errico, F. & Watts, I. Engraved ochres from the Middle Stone Age levels at Blombos Cave, South Africa. *J. Hum. Evol.* **57**, 27–47 (2009).
- Wadley, L. Ochre crayons or waste products? Replications compared with MSA 'crayons' from Sibudu cave, South Africa. *Before Farming* **2005**, 1–12 (2005).
- Rifkin, R. F. et al. Evaluating the photoprotective effects of ochre on human skin by in vivo SPF assessment: implications for human evolution, adaptation and dispersal. *PLoS ONE* **10**, e0136090 (2015).
- Joordens, J. C. et al. *Homo erectus* at Trinil on Java used shells for tool production and engraving. *Nature* **518**, 228–231 (2015).
- Mania, D. & Mania, U. Deliberate engravings on bone artefacts of *Homo erectus*. *Rock Art Res.* **5**, 91–107 (1988).
- Hovers, E., Vandermeersch, B. & Bar-Yosef, O. A Middle Palaeolithic engraved artefact from Qafzeh Cave, Israel. *Rock Art Res.* **14**, 79–87 (1997).
- Marshack, A. A Middle Paleolithic symbolic composition from the Golan heights: the earliest known depictive image. *Curr. Anthropol.* **37**, 357–365 (1996).
- Texier, P.-J. et al. The context, form and significance of the MSA engraved ostrich eggshell collection from Diepkloof Rock Shelter, Western Cape, South Africa. *J. Archaeol. Sci.* **40**, 3412–3431 (2013).
- Henshilwood, C. S. et al. Klipdrift Shelter, southern Cape, South Africa: preliminary report on the Howiesons Poort layers. *J. Archaeol. Sci.* **45**, 284–303 (2014).
- Rodríguez-Vidal, J. et al. A rock engraving made by Neanderthals in Gibraltar. *Proc. Natl Acad. Sci. USA* **111**, 13301–13306 (2014).
- Hoffmann, D. L. et al. U-Th dating of carbonate crusts reveals Neanderthal origin of Iberian cave art. *Science* **359**, 912–915 (2018).

22. Pearce, D. G. & Bonneau, A. Trouble on the dating scene. *Nat. Ecol. Evol.* **2**, 925–926 (2018).
23. Quiles, A. et al. A high-precision chronological model for the decorated Upper Paleolithic cave of Chauvet-Pont d'Arc, Ardèche, France. *Proc. Natl Acad. Sci. USA* **113**, 4670–4675 (2016).
24. Sadier, B. et al. Further constraints on the Chauvet cave artwork elaboration. *Proc. Natl Acad. Sci. USA* **109**, 8002–8006 (2012).
25. Pike, A. W. et al. U-series dating of Paleolithic art in 11 caves in Spain. *Science* **336**, 1409–1413 (2012).
26. Wendt, W. E. 'Art mobilier' from the Apollo 11 Cave, South West Africa: Africa's oldest dated works of art. *S. Afr. Archaeol. Bull.* **31**, 5–11 (1976).
27. Aubert, M. et al. Pleistocene cave art from Sulawesi, Indonesia. *Nature* **514**, 223–227 (2014).

Acknowledgements Partial funding for this research was provided to C.S.H., K.L.v.N. and F.d'E. by the Research Council of Norway through its Centres of Excellence funding scheme, Centre for Early Sapiens Behaviour (SapienCE), project number 262618; to C.S.H. by a South African National Research Foundation Research Chair (SARCH) at the University of the Witwatersrand and the Evolutionary Studies Institute at the University of the Witwatersrand, and the University of Bergen, Norway; F.d'E., L.D. and A.Q. by the LaScArBx, a research programme supported by the ANR (ANR-10-LABX-52). We thank C. Foster for the image in Fig. 2; P. Keene for assistance in the Cape Town laboratory, I. Svahn for assistance with electron microscopy in Bordeaux, G. Devilder for his input on Fig. 3 and M. Haaland for his stratigraphy image on Fig. 1.

Reviewer information Nature thanks J. C. A. Joordens, G. van den Bergh and the anonymous reviewer(s) for their contribution to the peer review of this work.

Author contributions C.S.H. and K.L.v.N. directed the excavations at Blombos Cave. C.S.H., F.d'E. and K.L.v.N. planned the methodology for examination of L13, and conceived and carried out the experimental replication tests. F.d'E. and L.D. carried out the microscopic analysis of L13 and experimental lines. L.D. carried out the chemical analyses of L13. A.Q. carried out the tribological analysis of the surfaces of L13 and produced the MP4 video (Supplementary Video) and three-dimensional PDF (Supplementary Data) of L13. L.P. recovered L13 during lithic analysis and recognized its importance. C.S.H., F.d'E., K.L.v.N., L.D. and A.Q. co-wrote the paper. L.P. contributed to editing the final paper.

Competing interests The authors declare no competing interests.

Additional information

Extended data is available for this paper at <https://doi.org/10.1038/s41586-018-0514-3>.

Supplementary information is available for this paper at <https://doi.org/10.1038/s41586-018-0514-3>.

Reprints and permissions information is available at <http://www.nature.com/reprints>.

Correspondence and requests for materials should be addressed to C.S.H.

Publisher's note: Springer Nature remains neutral with regard to jurisdictional claims in published maps and institutional affiliations.

METHODS

No statistical methods were used to predetermine sample size. The experiments were not randomized and investigators were not blinded to allocation during experiments and outcome assessment.

L13 was photographed using various macro-lenses, and examined and photographed with a motorized Leica Z6 APOA equipped with a DFC420 digital camera linked to LAS Montage and Leica Map DCM 3D computer software. Sections and three-dimensional models of selected portions of the lines on L13 were obtained with the LAS Montage, or by exporting depth maps obtained with the LAS Montage into the Leica Map DCM 3D. An image of the surface with the cross-hatching was obtained by importing overlapping micrographs from the LAS Montage into Adobe Illustrator and then producing a tracing of the red patches and other features identified on L13. This tracing was compared to the original under a microscope and corrected as required. Data on the morphology, size, number of patches composing the lines on L13 and presence of striations on these lines were recorded.

Unmodified pieces of ochre (Extended Data Fig. 7a) with narrow pointed or linear edges and variable texture and hardness were used to experimentally mark silcrete flakes (Extended Data Fig. 7b). These flakes are archaeological objects that derive from weathered and eroding MSA levels on the BBC talus.

The silcrete flakes were carefully cleaned with a brush under running water between marking experiments to remove all traces of ochre from their surfaces. In the first experiment, both pointed and linear ochre pieces were used to produce single- and multiple-stroke straight and curved lines. Multiple strokes were produced by repeatedly passing the ochre edge over the silcrete surface in the same direction or with a to-and-fro movement in an effort to accurately superimpose each new line on those previously made. In a second experiment, four pointed and four linear ochre edges were used to produce a sequence of six single-stroke, parallel, straight four-centimetre-long lines per edge (Supplementary Table 1).

The width and length of the microfacets created on the ochre pieces by the marking process and the maximum and minimum width of the lines produced on the silcrete flakes were measured with a digital calliper after each line was produced. In a third experiment, fine-grained ochre powder, produced by rubbing ochre pieces on a grindstone, was mixed with water in three different concentrations to produce three gradations of viscosity (thin, medium and thick).

Wooden sticks of 1 mm and 2 mm in diameter were gently crushed at one end with a hammer over a length of 1 cm to create a brush, and this was used to apply the three types of paint onto flat surfaces on the silcrete flakes.

The experimental lines made with the ochre pieces and wooden applicators were examined and photographed with the same equipment and procedures used for examining L13 immediately after their production and after being gently washed for 10 s under running tap water and dried at air temperature. This is the same cleaning process used for L13 and other BBC lithics recovered during sieving. When examining the experimental drawn and painted lines under the microscope, particular attention was paid to identifying features diagnostic of the marking technique, the direction in which the lines were made, the type of ochre edge used and the way in which washing altered the lines. In a final experiment, loose ochre powder produced by drawing nine four-centimetre-long straight lines with pointed and linear pieces on a silcrete flake was recovered and weighed on a scale with an accuracy of 1 mg.

Scanning electron microscopy with energy-dispersive X-ray spectroscopy (SEM–EDS) analyses were performed using a FEI Quanta 200. Back-scattered electron images (BSE) and elemental analyses were conducted under a low

vacuum mode with an accelerating voltage of 15 kV. BSE images were produced with a SiLi detector and EDS analyses with a SDD-EDAX detector. The EDS analyses were conducted under similar magnifications ($\times 50$, $\times 100$ or $\times 200$, and $\times 500$ or $\times 1,000$), at the same working distance (10 mm) and with the same acquisition time (100 s) for each EDS spectrum. Semi-quantitative data were calculated in weight percentages and normalized to 100%, C and O being included. Major ($>10\%$), minor ($>3\%$) and minor-to-trace elements ($<3\%$) were distinguished²⁸. For Raman analysis we used a SENTERRA dispersive Raman microscope (Bruker), equipped with an internal calibration system. The analyses were done with a 785-nm laser and a power of 1 mW to avoid transformation of mineral phases. Acquisition time was set to between 30 s and 70 s, and several co-additions of the signal if necessary. The working area was observed through the integrated colour camera, and data were collected with the software package OPUS 7.2.

High-resolution surface topography was acquired with a Sensofar S neox confocal microscope driven by SensoScan 6 software (Sensofar). For this study, we selected thirty 1.67×1.25 -mm areas that were measured with a $20\times$ objective (NA 0.45). This allowed for a spatial resolution of $0.65 \mu\text{m}$ and a vertical resolution of $0.31 \mu\text{m}$. Seven areas were measured outside of the red lines on the surface with the drawing, seven on the other surfaces of L13, ten on the knapped surfaces and ten on the natural cortical surfaces of two fine-grained silcrete flakes from the MSA levels at BBC (Extended Data Fig. 6a). Three-dimensional reconstructions of the measured areas were visually compared. The location of the measured areas on L13 was randomly selected (Extended Data Fig. 6c). Tribological analysis of these surfaces entailed pre-treatments and the calculation of surface texture parameters according to the ISO standard 25178, using the SensoMap software. Pre-treatments conducted on the raw acquisitions consisted of (1) filling non-measured points using the neighbourhood valid points algorithm, (2) removing the general shape of the surface by subtracting a second-degree polynomial, (3) separating waviness from roughness by the application of a Gaussian filter with a 0.25 -mm cut-off value, so that only roughness is kept for the calculation of surface texture parameters. Height, functional, spatial, hybrid and functional volume parameters were calculated for each quarter of each pre-treated area. Kruskal–Wallis multiple comparison tests²⁹ were applied to the dataset.

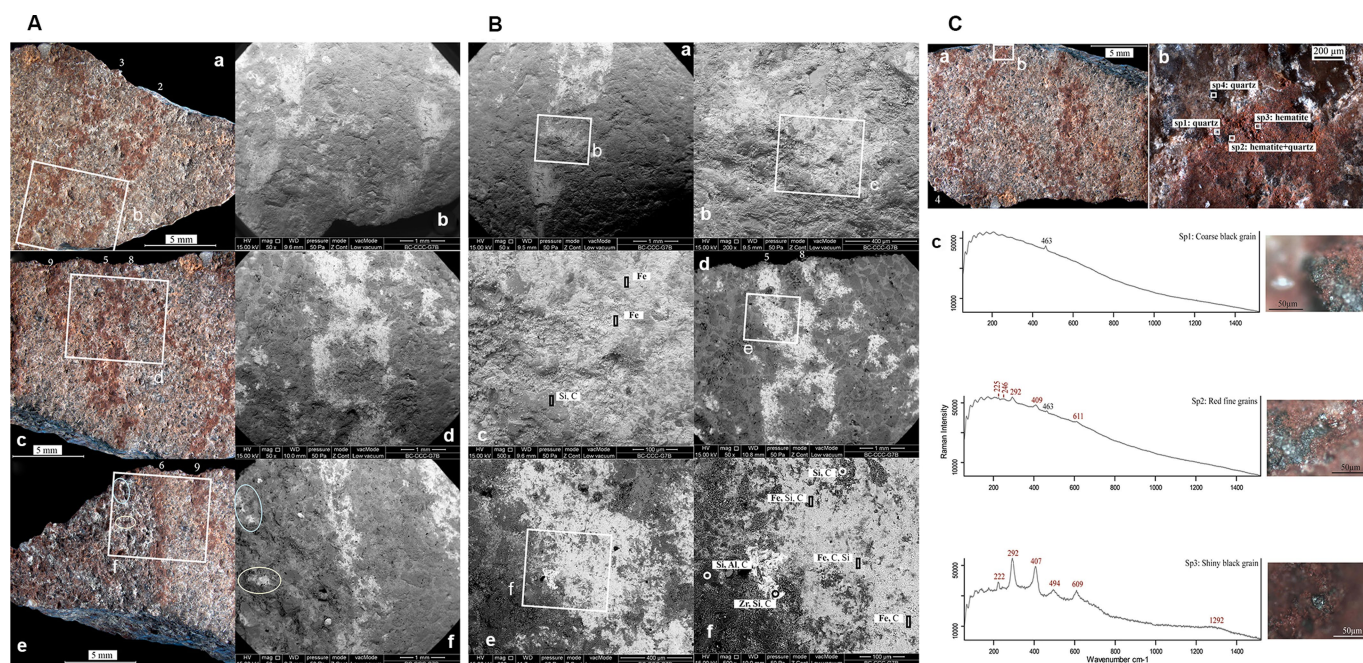
Scale sensitive fractal analysis using SensoMap 7.4.8443 software was also applied to L13³⁰. This analysis calculates the difference between the topographic surface and its planimetric area. The calculation is made at many consecutive scales by reducing the area of the triangles tiling the surface. Results are represented by an s-curve in which the rising indicates the scale at which the surface becomes rough.

A high-resolution three-dimensional model was created by photogrammetry using the Photoscan Standard software (Agisoft, version 1.4.0). Fifty-six photos taken with a macro lens from different points of view were processed to create the model and apply the texture (Supplementary Data and Supplementary Video).

Reporting summary. Further information on research design is available in the Nature Research Reporting Summary linked to this paper.

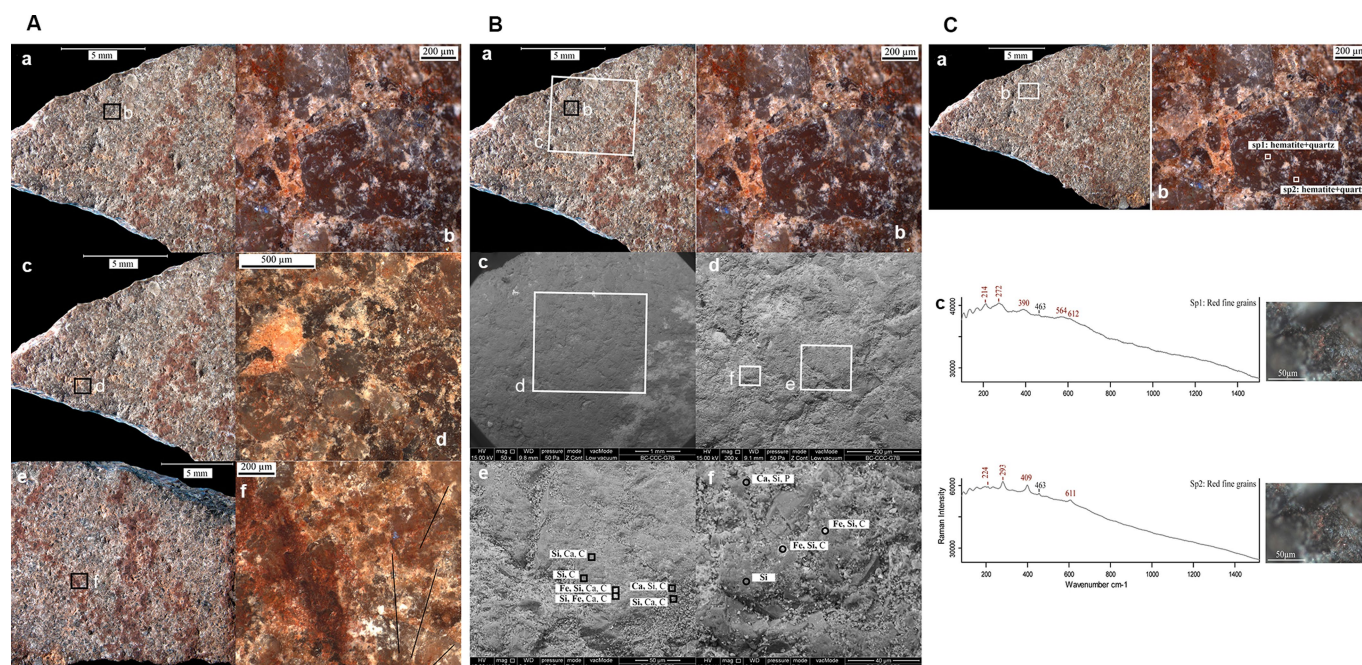
Data availability. All data generated or analysed during this study are included in the published article and its Supplementary Information.

28. d'Errico, F. et al. The technology of the earliest European cave paintings: El Castillo Cave, Spain. *J. Archaeol. Sci.* **70**, 48–65 (2016).
29. Siegel, S. & Castellan, N. J. Jr. *Nonparametric Statistics for the Behavioral Sciences* (McGraw-Hill, New York, 1988).
30. Brown, C. A. in *Characterisation of Areal Surface Texture* (ed. Leach, R.) 129–153 (Springer, Berlin, 2013).



Extended Data Fig. 1 | Microscopic examination and chemical analyses of the juxtaposed patches of red deposit that form the drawn lines on L13 and the smoothed surface of the silcrete flake. The lines consist mainly of fine-grained iron oxide (Fe), that were applied to the surface, as no haematite occur naturally in the silcrete raw material of L13. **A**, Photographs (left) and SEM-EDS images (right) of the red lines of the surface of L13. In the subpanels of **A**, images in **a**, **b** show lines 2 and 3; **c**, **d** show lines 5, 8 and 9; and **e**, **f** show lines 6 and 9 and red spots on a flake scar. The white rectangles in **a**, **c** and **e** indicate the areas that are enlarged in subpanels **b**, **d** and **f**, respectively. Notice the white appearance of the lines in the back-scattered electrons SEM-EDS images due to

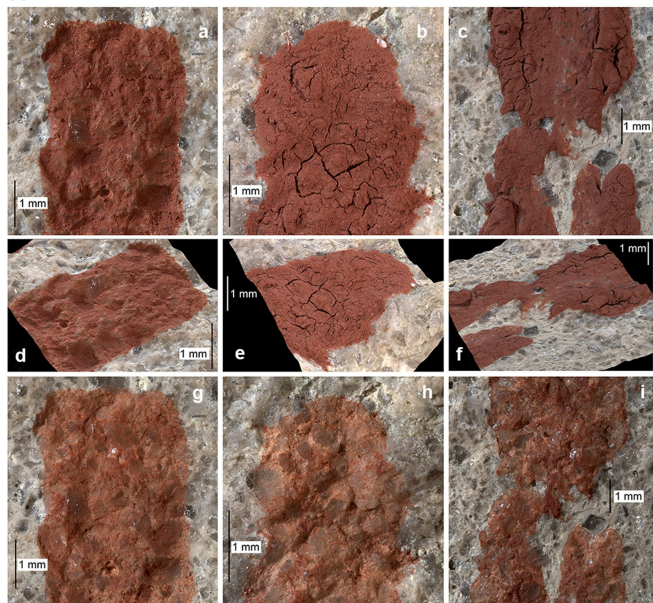
the presence of iron rich deposits. **B**, SEM-EDS images (back-scattered electrons) of line 2 and 5. Subpanels **a**–**c** show line 2; **d**–**f** show line 5. White squares indicate areas that are enlarged in the image with the corresponding letter. The rectangles and black/white circles in subpanels **c**, **f** show differences in elemental composition between the drawn lines (light areas) and the silcrete surface (dark areas). **C**, Raman analysis of line 4. Subpanel **a** shows a photograph with the location of the analysed area (white rectangle). Subpanel **b** shows the analysed spots and identified minerals. Subpanel **c** shows Raman spectra and micrographs of the analysed areas with peaks identifying haematite (red numbers) and quartz (black numbers).



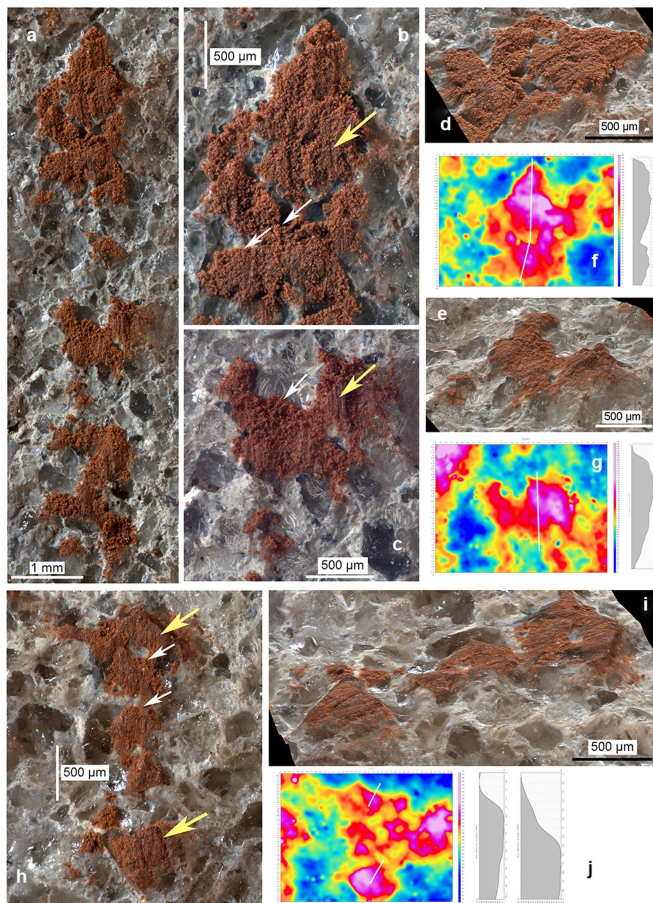
Extended Data Fig. 2 | Microscopic examination and chemical analyses of microresidues. The microresidues on the smoothed silcrete surface outside of the lines differ in Fe content from the red lines, which—along with the presence of microstriations—supports the theory that the silcrete flake was part of an ochre grindstone before the drawing was made. **A**, Photographs and micrographs of the lines drawn on L13. Black squares in subpanels **a**, **c**, **e** indicate the areas enlarged in the adjacent subpanels **b**, **d**, **f**. Red residues are clearly visible on the matrix and on quartz grains. **f**, Black lines highlight superficial randomly oriented striations. **B**, SEM-EDS analysis of the silcrete outside the drawn lines. In subpanels **a**, **c**, **d**, black and white squares indicate the areas enlarged in the adjacent

photograph. In subpanels **e**, **f**, the analysed spots (black squares and circles) identify the presence of isolated iron-rich particles on the surface of the matrix and the quartz grains. **C**, Raman analysis of microresidues preserved in quartz grain pits. Subpanel **a** shows a photograph with the location of the analysed area (white rectangle). Subpanel **b** shows analysed spots (white squares) and identified minerals. Subpanel **c** shows Raman spectra and micrographs of the analysed areas, with peaks identifying haematite (red numbers) and quartz (black numbers). The area shown in subpanel **b** of panel **C** is the same as the area shown in subpanel **b** of panel **B**.

A



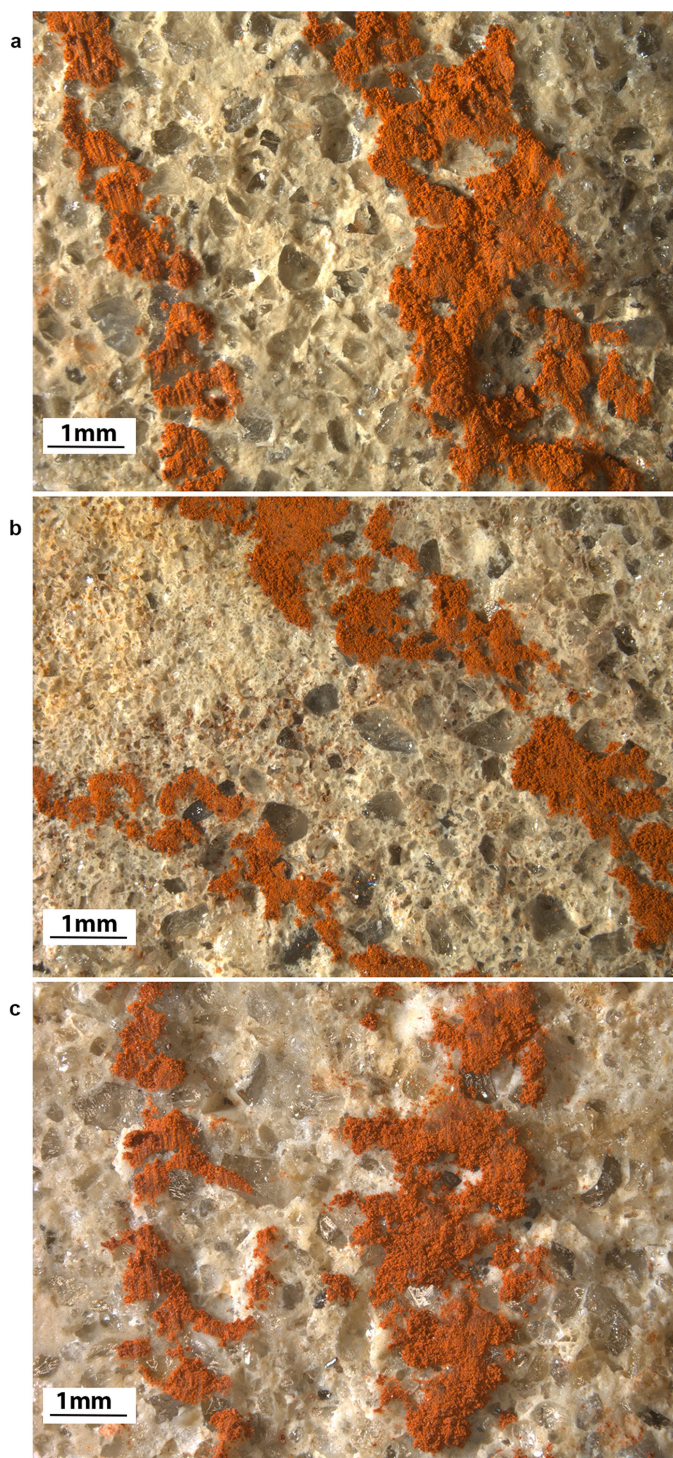
B



Extended Data Fig. 3 | See next page for caption.

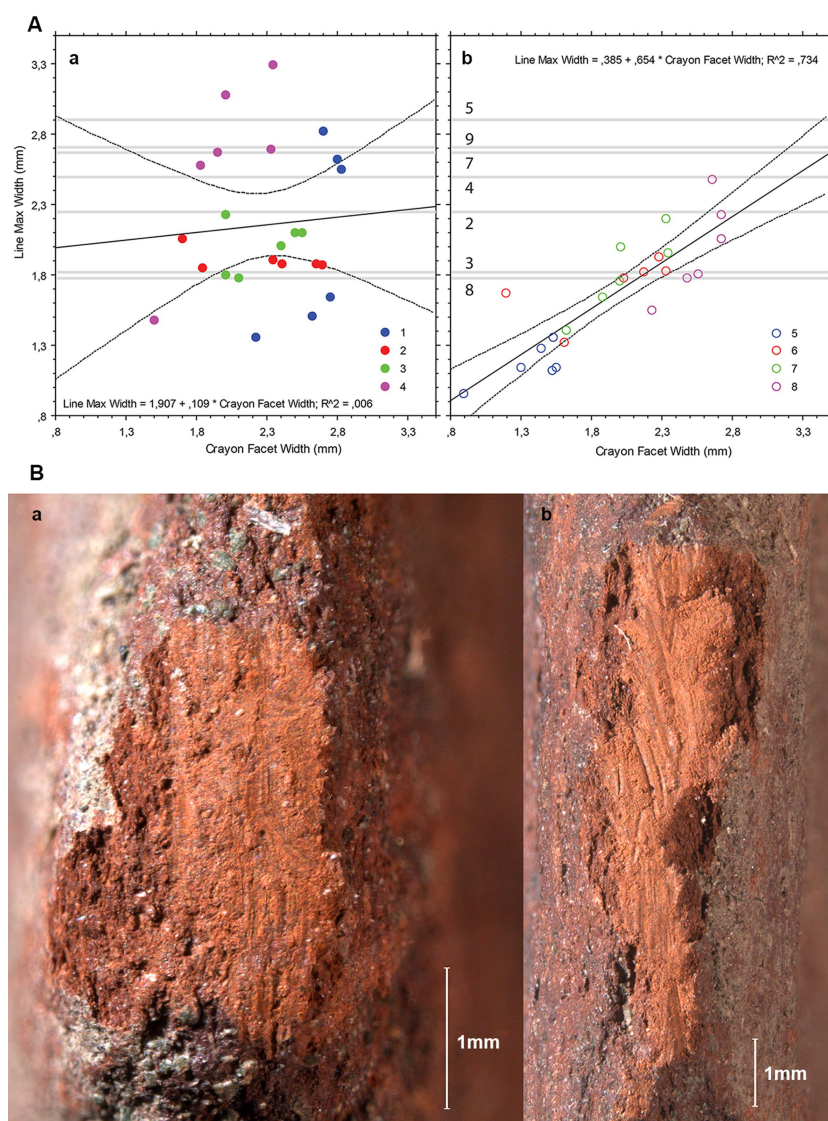
Extended Data Fig. 3 | Results from experimental marking of silcrete surfaces with ochre paint of varying viscosities and with an ochre crayon, and subsequent rinsing. **A**, Micrographs of experimentally painted lines before and after rinsing. Subpanels **a–c** show lines produced by applying a liquid (**a**), viscous (**b**) and very viscous (**c**) paint with a thin wooden brush on a silcrete surface. Subpanels **d–f** show the three-dimensional rendering of the same lines showing the surface topography. Subpanels **g–i** show the same lines after gently rinsing the surface of the silcrete under running tap water. **B**, Lines produced experimentally on a silcrete flake with an ochre crayon. Subpanel **a** shows a single-stroke line drawn from the top to the bottom. Subpanels **b, c** show close-up views and three-dimensional renderings (subpanels **d, e**) of selected areas of

subpanel **a**. Subpanels **h, i** show a photograph (**h**) and three-dimensional rendering (**i**) of a single-stroke line produced from the top to the bottom after gently rinsing the silcrete flake under running tap water. Subpanels **f, g** and **j** are depth maps and sections of **b, c** and a selected area of **h**, respectively. The locations of the sections are indicated on the depth maps by white bars. White arrows indicate deposits of powdery ochre preserved in recesses, and larger yellow arrows indicate prominent areas with compacted ochre deposits covered by striations. Compacted patches of ochre covered by striations and small deposits of ochre powder in recesses are preserved after the rinsing; these features and lines are similar to those on L13 (Fig. 4).



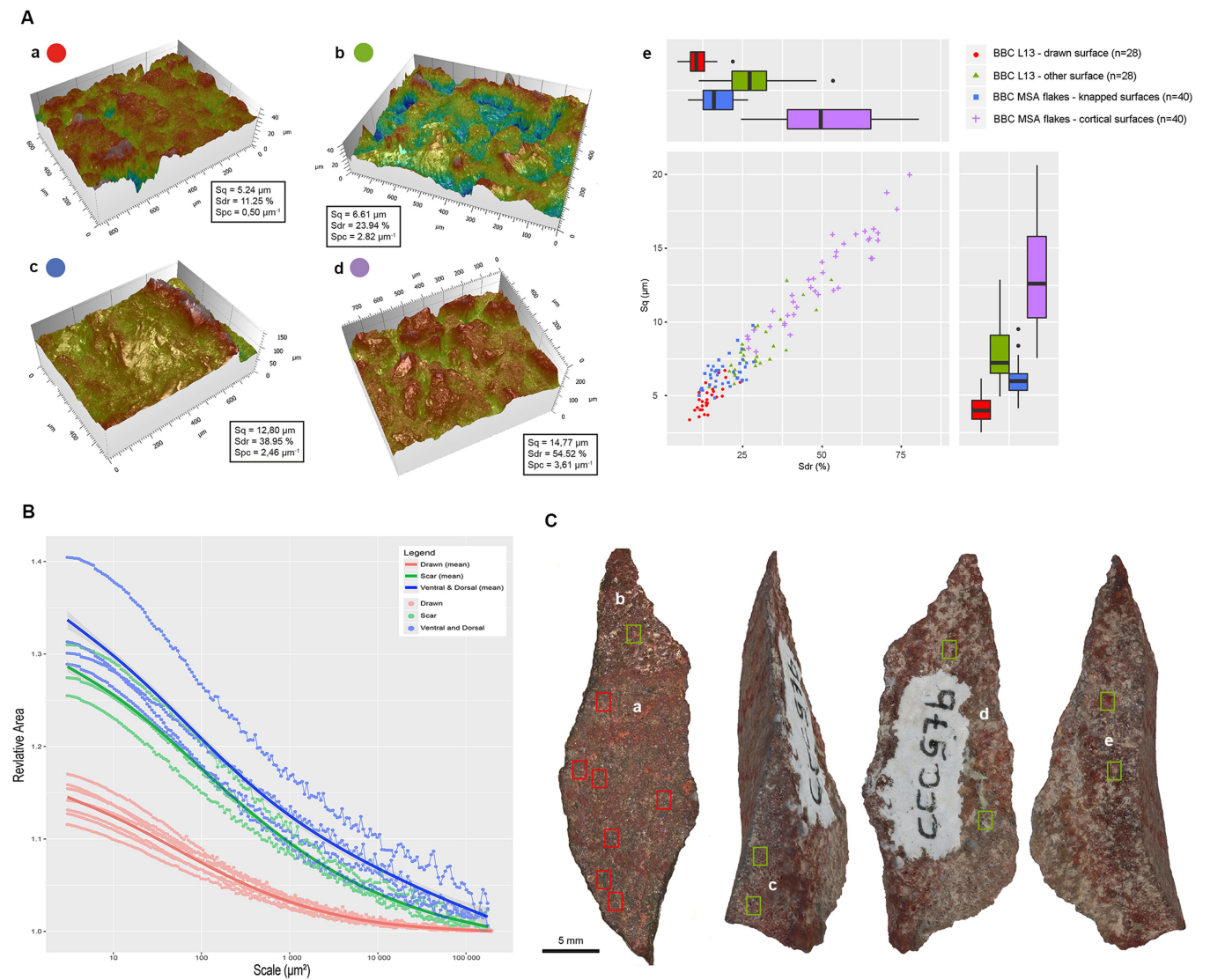
Extended Data Fig. 4 | Lines produced experimentally on silcrete flakes.

These images show that, as it is difficult to exactly superimpose a new line on a previous one, superimposing a line on a previous line generally results in a wider line. Unidirectional, superimposed lines retain the same features observed on a single-stroke line. Multiple lines produced by a to-and-fro movement of the ochre edge show microscopic evidence that the crayon was moved in both directions. **a**, Straight single- (left) and five-stroke line (right) produced from the top to the bottom. **b**, Curved single- (left) and five-stroke line (right) produced from top left to the bottom right. **c**, Straight single- (left) and five-stroke line (right) produced by a to-and-fro motion. The lines in this figure were not rinsed with water.



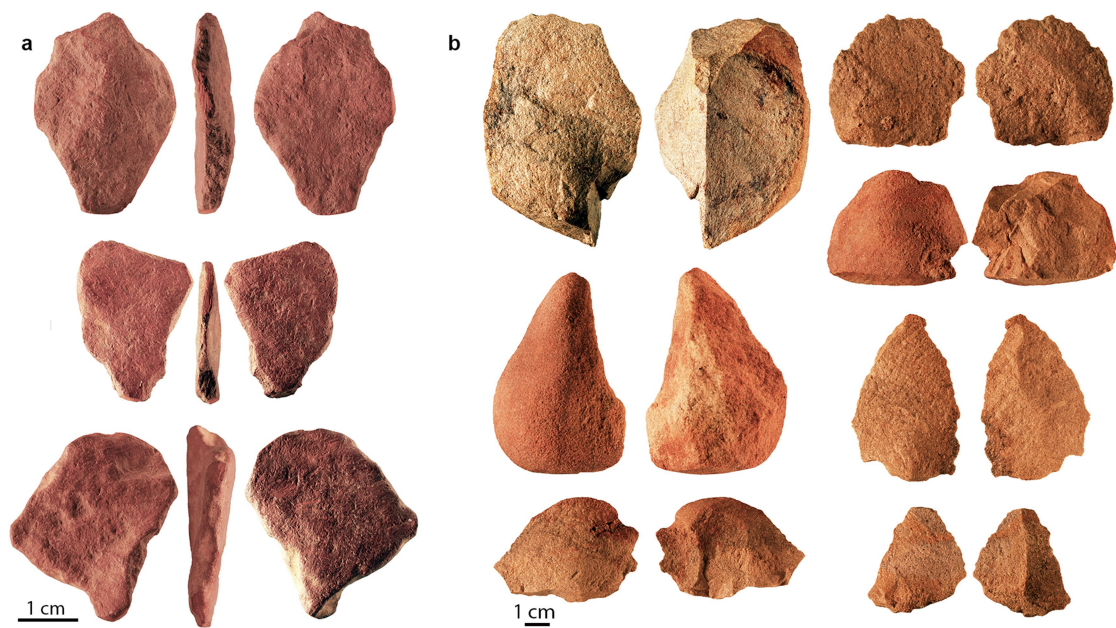
Extended Data Fig. 5 | Experimental marking of silcrete flakes with a variety of ochre crayons. The morphology of lines will depend on the properties and composition of the ochre, the roughness of the silcrete surface, the pressure exerted and the morphology of the ochre area in contact with the silcrete. In general, soft, plastic, clayish ochre will produce thicker and more continuous lines than silty or sand-rich ochre. Lines on fine-grained silcrete will be better defined than those on coarse silcrete. Stronger pressure will produce comparatively wider, thicker and better defined lines. Six lines made with each of eight unmodified ochre crayons had a maximum width ranging from about 0.9 to 3.3 mm. Lines produced with a pointed ochre crayon tend to be wider and more variable in width than those made with a linear edge. The width of lines made with a linear edge is strongly correlated with the maximum width of the facets on the ochre piece. By contrast, no correlation is observed between the lines

made with pointed crayons and the maximum width of the facets on the crayon. The width of the lines on the drawn cross-hatching present on L13 is comparable with that of the experimental lines. The range (1.8–2.9 mm) of this width best fits the width variability observed when marking the silcrete with a pointed crayon rather than an edge. This indicates that a pointed ochre crayon was used to produce the cross-hatching and that the facet of the crayon in contact with the silcrete was about 1.3–2.9 mm wide. **A**, Correlation between the width of lines and the width of the resulting facets on eight experimental ochre crayons. Subpanel **a** shows results from crayons with pointed active areas. Subpanel **b** shows results from crayons with linear active areas. The grey bars indicate the width of lines on L13. **B**, Wear facet appearing on the natural surface of an ochre crayon after a single stroke (subpanel **a**) and five strokes (subpanel **b**).



Extended Data Fig. 6 | Three-dimensional rendering of microscopic areas of L13 and silcrete flakes from BBC. Three-dimensional rendering shows flattening of the surface of L13 with the drawing, dissolution of the matrix between quartz grains on the cortex of the BBC silcrete flakes and an unworn appearance of the other surfaces of L13 and the ventral aspect of the BBC silcrete flakes. **A**, Roughness analysis of L13 and MSA silcrete flakes from BBC. Subpanels **a–d** show three-dimensional renderings of a selected area of the surface of L13 with the drawing (**a**), other surfaces of L13 (**b**), knapped (**c**) and cortical (**d**) surfaces of BBC silcrete flakes. Subpanel **e** shows box plots of the variation of roughness variables Sq and Sdr , and a bi-plot correlating these two variables. Notice the high degree of smoothness of the surface of L13 with the drawing relative to the other surfaces. A Kruskal–Wallis multiple comparison test demonstrates that

Sq , Sdr and Spc on the surface with the drawing are significantly lower ($P < 0.01$) than those measured on the remainder of the analysed surfaces of L13. **B**, Areal fractal analysis confirms a clear difference in roughness between the surface with the drawing and other surfaces of L13. This is consistent with the interpretation of the wear on the surface with the drawing as being produced by grinding activities before the drawing occurred. **C**, Analysis of L13 with confocal microscopy. Rectangles indicate the locations of the analysed areas on the surface with the drawing (red) and on the other surfaces (green). Letters distinguish analyses conducted with areal fractal analysis on the surface with the drawing (**a**), a flake scar on the surface with the drawing (**b**), a flake scar on the dorsal surface (**c**) from analyses made on the dorsal (**d**) and ventral surfaces (**e**).



Extended Data Fig. 7 | Ochre and silcrete used in the replication experiments. a, Pieces of ochre used experimentally to produce lines on silcrete flakes. **b,** Silcrete flakes used during the experiments.

Life Sciences Reporting Summary

Nature Research wishes to improve the reproducibility of the work that we publish. This form is intended for publication with all accepted life science papers and provides structure for consistency and transparency in reporting. Every life science submission will use this form; some list items might not apply to an individual manuscript, but all fields must be completed for clarity.

For further information on the points included in this form, see [Reporting Life Sciences Research](#). For further information on Nature Research policies, including our [data availability policy](#), see [Authors & Referees](#) and the [Editorial Policy Checklist](#).

Please do not complete any field with "not applicable" or n/a. Refer to the help text for what text to use if an item is not relevant to your study. For final submission: please carefully check your responses for accuracy; you will not be able to make changes later.

► Experimental design

1. Sample size

Describe how sample size was determined.

The entire surface of the archaeological object described in our manuscript was analysed and all the lines present on it were examined and documented. Thus, the sample size corresponds to the sum of all lines available for study. The same applies to the experimental lines that we made and all these were analyzed

2. Data exclusions

Describe any data exclusions.

No data were excluded from the analysis

3. Replication

Describe the measures taken to verify the reproducibility of the experimental findings.

Raman and SEM analyses of residues, and roughness measurements, both inside and outside the drawn lines on the object were conducted in as many places as possible. In the analyses of the archaeological object reproducibility was ensured by repeating analyses at different locations. However, the number of these analyses were circumscribed by the relatively small size of the object, the fact that a relatively large area on one of its aspects is covered by a white 'varnish', the state of preservation of the surface as well as for conservation reasons. The sample size of the experimental lines was determined by availability of silcrete flakes, similar in size to L13, that were recovered on the Blombos Cave MSA talus and were out of context. For conservation reasons we were not able to use plotted flakes recovered in situ. These out of context silcrete flakes had suitable granulometry on which to conduct the experiments. The number of roughness analyses on these flakes was determined by the number of spots analyzed on the archaeological object in order to contrast comparable samples. In the case of the experimental lines two sub-populations of 24 lines (SI Table 1, SI figure 4) were considered sufficient to identify the degree of correlation between the line width and the crayon facet width.

4. Randomization

Describe how samples/organisms/participants were allocated into experimental groups.

Each new set of experimental lines was made on the available silcrete flakes that randomly came out of Blombos Cave deposits that were leaching onto the talus

5. Blinding

Describe whether the investigators were blinded to group allocation during data collection and/or analysis.

The investigators were not blinded during the collection and analysis of data

Note: all in vivo studies must report how sample size was determined and whether blinding and randomization were used.

6. Statistical parameters

For all figures and tables that use statistical methods, confirm that the following items are present in relevant figure legends (or in the Methods section if additional space is needed).

n/a Confirmed

- ☐ ☒ The exact sample size (*n*) for each experimental group/condition, given as a discrete number and unit of measurement (animals, litters, cultures, etc.)
- ☐ ☒ A description of how samples were collected, noting whether measurements were taken from distinct samples or whether the same sample was measured repeatedly
- ☐ ☒ A statement indicating how many times each experiment was replicated
- ☐ ☒ The statistical test(s) used and whether they are one- or two-sided
Only common tests should be described solely by name; describe more complex techniques in the Methods section.
- ☒ ☐ A description of any assumptions or corrections, such as an adjustment for multiple comparisons
- ☐ ☒ Test values indicating whether an effect is present
*Provide confidence intervals or give results of significance tests (e.g. *P* values) as exact values whenever appropriate and with effect sizes noted.*
- ☒ ☐ A clear description of statistics including central tendency (e.g. median, mean) and variation (e.g. standard deviation, interquartile range)
- ☐ ☒ Clearly defined error bars in all relevant figure captions (with explicit mention of central tendency and variation)

See the web collection on [statistics for biologists](#) for further resources and guidance.

► Software

Policy information about [availability of computer code](#)

7. Software

Describe the software used to analyze the data in this study.

The softwares we used are available end-user applications. They were applied to increase focus when taking photos under the microscope and to produce 3D reconstructions (LAS Montage and Leica Map DCM 3D software); produce tracings from photos (Adobe Illustrator), visualize and compare Raman spectra (OPUS 7.2.); visualize and store surface data obtained with a confocal microscope (SensoScan 6); conduct scale sensitive fractal analysis (SSFA) using SensoMap 7.4.8443 on these data; and create by photogrammetry a 3D model of the archaeological object (Agisoft 1.2.5)

For manuscripts utilizing custom algorithms or software that are central to the paper but not yet described in the published literature, software must be made available to editors and reviewers upon request. We strongly encourage code deposition in a community repository (e.g. GitHub). *Nature Methods* [guidance for providing algorithms and software for publication](#) provides further information on this topic.

► Materials and reagents

Policy information about [availability of materials](#)

8. Materials availability

Indicate whether there are restrictions on availability of unique materials or if these materials are only available for distribution by a third party.

The archaeological object described in our manuscript is unique. All archaeological material recovered from Blombos Cave is stored and curated, after study, at the IZIKO South African Museum, Cape Town and is available for study there.

9. Antibodies

Describe the antibodies used and how they were validated for use in the system under study (i.e. assay and species).

not applicable

10. Eukaryotic cell lines

a. State the source of each eukaryotic cell line used.

not applicable

b. Describe the method of cell line authentication used.

not applicable

c. Report whether the cell lines were tested for mycoplasma contamination.

not applicable

d. If any of the cell lines used are listed in the database of commonly misidentified cell lines maintained by [ICLAC](#), provide a scientific rationale for their use.

not applicable

► Animals and human research participants

Policy information about [studies involving animals](#); when reporting animal research, follow the [ARRIVE guidelines](#)

11. Description of research animals

Provide all relevant details on animals and/or animal-derived materials used in the study.

not applicable

Policy information about [studies involving human research participants](#)

12. Description of human research participants

Describe the covariate-relevant population characteristics of the human research participants.

Four researchers, co-authors of the manuscript (CH, FdE, LD, AQ) were involved in the experiments. In archaeology it is common practice that experiments requiring a specialized expertise in prehistoric technology are conducted by the researchers themselves.